

NONLINEAR CONTROL OF 3-D OVERHEAD CRANES: ENERGY-BASED DECOUPLING

Dongkyoung Chwa^a and Keum-Shik Hong^b

^a School of Electrical and Computer Engineering, Ajou University, Suwon, Korea

^b School of Mechanical Engineering, Pusan National University, Busan, Korea
e-mail: dkchwa@ajou.ac.kr, kshong@pusan.ac.kr

Abstract: In this paper, a nonlinear anti-sway control law for overhead cranes is investigated. The crane model itself is adopted from the literature; however, a new nonlinear decoupling control law that provides superior position-regulation and sway-suppression characteristics is proposed in this paper. The derived control law uses the sway angular rate as well as the sway angle as feedback. The performance of the proposed control law is compared with those of the PD and E^2 control laws in the literature. The transient characteristics of the proposed control law are also verified using a 3-D pilot crane. Simulation and experimental results are discussed. *Copyright © 2005 IFAC*

Keywords: nonlinear control, modelling, decoupling, regulation, Lyapunov function.

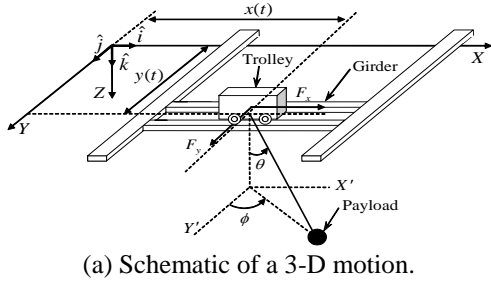
1. INTRODUCTION

Cranes can be categorized into four types: overhead cranes, container cranes, tower cranes, and jib cranes. This paper focuses on overhead cranes that are widely used in factories and warehouses (Butler et al., 1991). A major difference between container cranes and overhead cranes is that there is no girder motion in container cranes; that is, the trolley motion is the only motion that makes the load swing, whereas in overhead cranes, both the trolley and girder motions may occur at the same time. Hence, in container cranes, the sway motion is assumed to occur in a plane, whereas the sway motion of overhead cranes should be analyzed in three-dimensional space.

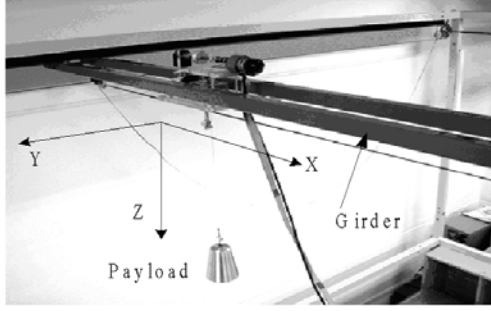
For the speed control of a trolley in two-dimensional space, an analytical time-optimal control solution without a hoisting motion was investigated by Manson (1977). In contrast to speed control, the torque control method applies control forces/torques in such a way that the dynamics of the controlled system meet a given reference signal. The torque control method is more attractive from the aspects of accuracy and energy saving. Moustafa and Ebeid (1988) derived a 3-D nonlinear model of overhead cranes and investigated a linear state feedback

control by linearizing the derived 3-D model. In (Hong, *et al*, 2000), to achieve both fast traveling of the trolley and precise regulation of the sway motion at the end of trolley strokes, a two stage control combining a time-optimal traveling control and a variable structure control for residual sway suppression was proposed. Fang, Dixon, Dawson, and Zergeroglu (2003) investigated a nonlinear control based upon the total energy of a 3-D overhead crane.

In this paper, an energy-based (Lyapunov-function-based) nonlinear control design for a 3-D crane is investigated. The advantage of using an energy-based control is that the nonlinearity of the plant can be fully incorporated into control law design when the energy function is differentiated along the plant dynamics. Also, the uniform asymptotic stability of the closed-loop system can be guaranteed by a properly chosen energy function. However, the disadvantage of energy-based control is that it is difficult to improve the transient performance (i.e., rise time, settling time, etc.) in a systematic way even though its stability is assured. Hence, a trial and error approach to improve the transient performance is normally pursued. The contributions of this paper are the following. An energy-based control law with



(a) Schematic of a 3-D motion.



(b) A 3-D pilotcrane: InTeCo (Poland).

Fig. 1. 3-D overhead crane: its schematic and a pilot crane for experiment.

improved rise time and sway suppression capability for a 3-D crane is proposed. The uniform asymptotic stability of the closed-loop system is assured. Finally, the developed algorithm is verified through simulations and experiments using a 3-D pilot crane.

2. SYSTEM DYNAMICS

For the successful suppression of the sway motion of a suspended load, it is important to know what part of the crane dynamics should be included in the control law design stage and what part can be neglected. In the case of overhead cranes, in contrast to container cranes, a three-dimensional model should be used to represent the swing dynamics of the suspended load. In this study, the model developed in (Moustafa, and Ebeid, 1988) and (Fang, *et al.*, 2003) was adopted.

Fig. 1 shows the schematic of a 3-D overhead crane. Let X be the trolley moving direction and Y be the girder moving direction. Let ϕ be the angle of the Y' -axis and the projected line of the rope to the $X' - Y'$ plane. Let θ be the angle between the vertical line and the rope. Let $x(t)$, $y(t) \in R$ be the displacements of the trolley and the girder, respectively. Let F_x and F_y be the control forces applied to the trolley and the girder, respectively.

The following assumptions are made: i) payload and trolley are connected by a massless rigid rod; that is, a pendulum motion of the load is considered; ii) the trolley and girder masses and the positions of the trolley and girder are exactly known; iii) the ball joint connecting the rod and trolley is frictionless and this joint does not rotate about the connecting rod; iv) the rod elongation is negligible; v) the rod length

(hoist rope length) is constant, which gives a four-d.o.f. crane model rather than five. Now, a variable $q(t) \in R^4$ is defined as $q(t) = [x(t), y(t), \theta(t), \phi(t)]^T$.

In accordance with the assumptions made above, the crane dynamics are given by

$$M(q)\ddot{q} + V_m(q, \dot{q})\dot{q} + G(q) = u \quad (1)$$

where

$$M = \begin{pmatrix} m_{11} & 0 & m_{13} & m_{14} \\ 0 & m_{22} & m_{23} & m_{24} \\ m_{31} & m_{32} & m_{33} & 0 \\ m_{41} & m_{42} & 0 & m_{44} \end{pmatrix}, \quad V_m = \begin{pmatrix} 0 & 0 & V_{m13} & V_{m14} \\ 0 & 0 & V_{m23} & V_{m24} \\ 0 & 0 & 0 & V_{m34} \\ 0 & 0 & V_{m43} & V_{m44} \end{pmatrix}$$

$$G = [0 \quad 0 \quad m_p g L \sin \theta \quad 0]^T$$

$$m_{11} = m_p + m_r + m_c, \quad m_{13} = m_p L \cos \theta \sin \phi$$

$$m_{14} = m_p L \sin \theta \cos \phi, \quad m_{22} = m_p + m_c$$

$$m_{23} = m_p L \cos \theta \cos \phi, \quad m_{24} = -m_p L \sin \theta \sin \phi$$

$$m_{31} = m_p L \cos \theta \sin \phi, \quad m_{32} = m_p L \cos \theta \cos \phi$$

$$m_{33} = m_p L^2 + I, \quad m_{41} = m_p L \sin \theta \cos \phi$$

$$m_{42} = -m_p L \sin \theta \sin \phi, \quad m_{44} = m_p L^2 \sin^2 \theta + I$$

$$V_{m13} = -m_p L \sin \theta \sin \phi \dot{\theta} + m_p L \cos \theta \cos \phi \dot{\phi}$$

$$V_{m14} = m_p L \cos \theta \cos \phi \dot{\theta} - m_p L \sin \theta \sin \phi \dot{\phi}$$

$$V_{m23} = -m_p L \sin \theta \cos \phi \dot{\theta} - m_p L \cos \theta \sin \phi \dot{\phi}$$

$$V_{m24} = -m_p L \cos \theta \sin \phi \dot{\theta} - m_p L \sin \theta \cos \phi \dot{\phi}$$

$$V_{m34} = -m_p L^2 \sin \theta \cos \theta \dot{\phi}, \quad V_{m43} = m_p L^2 \sin \theta \cos \theta \dot{\phi}$$

$$V_{m44} = m_p L^2 \sin \theta \cos \theta \dot{\theta}.$$

In the above expressions, m_p , m_g , and m_t are the payload mass, girder mass, and trolley mass, respectively; I is the mass moment of inertia of the payload; L is the length of the suspending rope; g is the gravitational acceleration. It is remarked that the inertia matrix and centripetal term, $M(q)$ and $V_m(q, \dot{q})$, satisfy the skew-symmetric relationship of $\xi^T (\dot{M}(q)/2 - V_m(q, \dot{q})) \xi = 0$ where $\dot{M}(q)$ is the time derivative of $M(q)$, and that they hold the inequalities $k_1 \|\xi\|^2 \leq \xi^T M(q) \xi \leq k_2 \|\xi\|^2$ for $\xi \in R^4$.

To decouple the x - and y -dynamics from the θ - and ϕ -dynamics, (1) is rewritten as

$$\ddot{q} = M^{-1}(q)\{u - V_m(q, \dot{q})\dot{q} - G(q)\}. \quad (2)$$

Then, the x - and y -dynamics are

$$\ddot{r} = (PF + W)/\det(M). \quad (3)$$

where $r = [x \quad y]^T$, $P = \begin{pmatrix} p_{11} & p_{12} \\ p_{12} & p_{22} \end{pmatrix} > 0$,

$F = [F_x \quad F_y]^T$, $W = [w_1 \quad w_2]^T$, $\det(M)$ stands for the determinant of $M(q)$. Expression for p_{ij} and w_k for $1 \leq i, j, k \leq 2$ are referred to (Fang, *et al.*, 2003).

Finally, the θ - and ϕ -dynamics are

$$\begin{pmatrix} \ddot{\theta} \\ \ddot{\phi} \end{pmatrix} = \begin{pmatrix} m_{33} & 0 \\ 0 & m_{44} \end{pmatrix}^{-1} \cdot \left\{ - \begin{pmatrix} m_{31} & m_{32} \\ m_{41} & m_{42} \end{pmatrix} \cdot \begin{pmatrix} \ddot{x} \\ \ddot{y} \end{pmatrix} \right\} \quad (4)$$

$$-\begin{pmatrix} 0 & V_{m34} \\ V_{m43} & V_{m44} \end{pmatrix} \cdot \begin{pmatrix} \dot{\theta} \\ \dot{\phi} \end{pmatrix} - \begin{pmatrix} m_p g L \sin \theta \\ 0 \end{pmatrix} \Bigg\}$$

3. CONTROL LAW DESIGN

In this section, a nonlinear control law for suppressing the sway angle of the suspended load is derived. The novelty of this law lies in improving the transient performance. The information on the sway angle, sway angular velocity, trolley displacement and velocity, girder displacement and velocity is assumed to be known (the sway angular velocity can be observed in practice, but this is not an issue in this paper). For comparison purposes, after introducing the PD and E^2 coupling control laws of Fang *et al.* (2003), a variant form of the nonlinear control law that is superior to the PD and E^2 control laws is proposed. Let the position error be defined by

$$e = r - r_d = [x_e \quad y_e]^T \quad (5)$$

where $r_d = [x_d \quad y_d]^T$, $x_e = x - x_d$, $y_e = y - y_d$, and x_d and y_d are the desired trolley and girder positions, respectively.

(i) The PD control law in (Kiss, Levine, and Mullhaupt, 2000) and (Fang, *et al.*, 2003) is in the form of

$$F = (-k_p e - k_d \dot{e}) / k_E \quad (6)$$

where k_E , k_p , and k_d are positive constants.

(ii) The E^2 coupling control law of (Fang, *et al.*, 2003) is given by

$$F = [\Omega]^{-1} \left(-k_p e - k_d \dot{e} - \frac{k_v}{\det(M)} W \right) \quad (7)$$

where $\Omega = k_E E I_2 + \frac{k_v}{\det(M)} P \in R^{2 \times 2}$, $E(q, \dot{q}) =$

$\dot{q}^T M(q) \dot{q} / 2 + m_p g L (1 - \cos(\theta))$, and I_2 is a 2×2 identity matrix.

(iii) To improve the transient performance in sway suppression and the robustness against initial swing and varying payload, the following new control law is proposed:

$$F = \left[\frac{P}{\det(M)} \right]^{-1} \cdot \left(-e - 2\dot{e} - \frac{W}{\det(M)} + \begin{pmatrix} \sin \phi \\ \cos \phi \end{pmatrix} \cdot f \right) \quad (8)$$

where

$$f = L \sin \theta (\dot{\phi})^2 + \sqrt{\bar{a}} \dot{\theta} + \bar{f}, \quad (9)$$

$$\bar{a} = \{ \cos \theta m_p L / (m_p L^2 + I) \}^2, \quad (10)$$

$$\bar{f} = \begin{cases} \text{i) } [\sqrt{\bar{a}} \dot{\theta} - \{ \sin \phi (\dot{x}_e + x_e) + \cos \phi (\dot{y}_e + y_e) \}]^{-1} \\ \quad \cdot [\{ \sin \phi (\dot{x}_e + x_e) + \cos \phi (\dot{y}_e + y_e) \} \\ \quad \cdot L \sin \theta (\dot{\phi})^2 + (\sin \phi \dot{x}_e + \cos \phi \dot{y}_e) \cdot \sqrt{\bar{a}} \dot{\theta}], \\ \text{ii) } \text{sgn}(\dot{\theta}) \cdot | \sin \phi (2\dot{x}_e + x_e) + \cos \phi (2\dot{y}_e + y_e) |, \\ \text{iii) } \text{if } \sqrt{\bar{a}} \dot{\theta} - \{ \sin \phi (\dot{x}_e + x_e) + \cos \phi (\dot{y}_e + y_e) \} = 0 \\ \quad \text{and } \cos \phi (\dot{x}_e + x_e) - \sin \phi (\dot{y}_e + y_e) \neq 0, \end{cases}$$

$$\bar{f} = \begin{cases} \text{iii) } \sin \phi \dot{x}_e + \cos \phi \dot{y}_e, \\ \text{if } \sqrt{\bar{a}} \dot{\theta} - \{ \sin \phi (\dot{x}_e + x_e) + \cos \phi (\dot{y}_e + y_e) \} = 0 \text{ (11)} \\ \quad \text{and } \cos \phi (\dot{x}_e + x_e) - \sin \phi (\dot{y}_e + y_e) = 0. \end{cases}$$

Theorem 1: Consider the plant (3)-(4) with $|\theta(0)| < \pi/2$, and the control law given by (8)-(11). Then, the trolley and girder position errors x_e and y_e , and the swing angle θ , converge to zero asymptotically, and $\dot{q} = [\dot{x} \quad \dot{y} \quad \dot{\theta} \quad \dot{\phi}]^T$ remains bounded for all $t \geq 0$.

Proof: By substituting (8) into (3) and rearranging the terms, the position error dynamics become

$$\ddot{e} + 2\dot{e} + e = \begin{pmatrix} \sin \phi \\ \cos \phi \end{pmatrix} \cdot f \quad (12)$$

where $e = r - r_d$, in which the target trolley and girder positions, x_d and y_d , are constants. The θ -dynamics in (4) become

$$(m_p L^2 + I) \ddot{\theta} + (\cos \theta \sin \phi \ddot{x} + \cos \theta \cos \phi \ddot{y}) m_p L - m_p L^2 \sin \theta \cos \theta (\dot{\phi})^2 + m_p g L \sin \theta = 0 \quad (13)$$

or

$$(m_p L^2 + I) \ddot{\theta} + \{ \sin \phi (-2\dot{x}_e - x_e) + \cos \phi (-2\dot{y}_e - y_e) + f \} \cos \theta m_p L - m_p L^2 \sin \theta \cos \theta (\dot{\phi})^2 + m_p g L \sin \theta = 0. \quad (14)$$

Rewriting of (12) and (14) yields:

$$\ddot{x}_e + 2\dot{x}_e + x_e = \sin \phi \cdot f, \quad (15)$$

$$\ddot{y}_e + 2\dot{y}_e + y_e = \cos \phi \cdot f, \quad (16)$$

$$(m_p L^2 + I) \cdot \{ \ddot{\theta} + \bar{a} \dot{\theta} \} + m_p g L \sin \theta = \{ \sin \phi (2\dot{x}_e + x_e) + \cos \phi (2\dot{y}_e + y_e) \} \cos \theta m_p L - \bar{f} \cos \theta m_p L. \quad (17)$$

It is remarked that only (15)-(17) are used in control law design, because the ϕ -dynamics become insignificant if θ converges to zero; see (Fang, *et al.*, 2003).

First, a positive definite function for the x - and y -dynamics is considered as follows:

$$V_1 = (\dot{e} + e)^T (\dot{e} + e) / 2. \quad (18)$$

Then, the time derivative of (18) using (15)-(16) becomes

$$\begin{aligned} \dot{V}_1 &= (\dot{e} + e)^T (\ddot{e} + \dot{e}) \\ &= -(\dot{e} + e)^T (\dot{e} + e) + \{ \sin \phi (\dot{x}_e + x_e) \\ &\quad + \cos \phi (\dot{y}_e + y_e) \} f. \end{aligned} \quad (19)$$

Also, the sway dynamics, (17), are expressed as

$$\begin{aligned} \dot{\theta}_1 &= \theta_2 \\ \dot{\theta}_2 &= -\bar{a} \theta_2 - \bar{c} \sin(\theta_1) + \{ \sin \phi (2\dot{x}_e + x_e) \\ &\quad + \cos \phi (2\dot{y}_e + y_e) \} \cdot \sqrt{\bar{a}} - \sqrt{\bar{a}} \cdot \bar{f} \end{aligned} \quad (20)$$

where $\theta_1 = \theta$, $\theta_2 = \dot{\theta}$, and $\bar{c} = m_p g L / (m_p L^2 + I)$. An energy function for system (20) (i.e., a positive definite function for the θ -dynamics) is considered as follows:

$$V_2 = 1/2 \cdot \theta_2^2 + \bar{c} \{ 1 - \cos \theta_1 \}. \quad (21)$$

Then, the time derivative of (21) using (20) becomes

$$\begin{aligned}\dot{V}_2 &= \theta_2 \dot{\theta}_2 + \bar{c} \sin(\theta_1) \dot{\theta}_1 \\ &= -\bar{a} \theta_2^2 + \{\sin \phi (2\dot{x}_e + \dot{x}_e) + \cos \phi (2\dot{y}_e + \dot{y}_e)\} \\ &\quad \cdot \sqrt{\bar{a}} \theta_2 - \sqrt{\bar{a}} \theta_2 \cdot \bar{f}.\end{aligned}\quad (22)$$

Then, using the relationship

$$\begin{aligned}(\dot{e} + e)^T (\dot{e} + e) &= \{\sin \phi (\dot{x}_e + x_e) + \cos \phi (\dot{y}_e + y_e)\}^2 \\ &\quad + \{\cos \phi (\dot{x}_e + x_e) - \sin \phi (\dot{y}_e + y_e)\}^2,\end{aligned}\quad (23)$$

the time derivative of $V = V_1 + V_2$ becomes

$$\begin{aligned}\dot{V} &\leq -\{\sin \phi (\dot{x}_e + x_e) + \cos \phi (\dot{y}_e + y_e)\}^2 \\ &\quad - \{\cos \phi (\dot{x}_e + x_e) - \sin \phi (\dot{y}_e + y_e)\}^2 - \bar{a} \theta_2^2 \\ &\quad + \{\sin \phi (\dot{x}_e + x_e) + \cos \phi (\dot{y}_e + y_e)\} \cdot (f + \sqrt{\bar{a}} \theta_2) \\ &\quad + (\sin \phi \dot{x}_e + \cos \phi \dot{y}_e) \cdot \sqrt{\bar{a}} \theta_2 - \sqrt{\bar{a}} \theta_2 \cdot \bar{f} \\ &\leq -\{\sin \phi (\dot{x}_e + x_e) + \cos \phi (\dot{y}_e + y_e) - \sqrt{\bar{a}} \theta_2\}^2 \\ &\quad - \{\cos \phi (\dot{x}_e + x_e) - \sin \phi (\dot{y}_e + y_e)\}^2 \\ &\quad + [\{\sin \phi (\dot{x}_e + x_e) + \cos \phi (\dot{y}_e + y_e)\} \cdot L \sin \theta (\dot{\phi})^2 \\ &\quad + (\sin \phi \dot{x}_e + \cos \phi \dot{y}_e) \cdot \sqrt{\bar{a}} \theta_2] \\ &\quad - \{\sqrt{\bar{a}} \theta_2 - \sin \phi (\dot{x}_e + x_e) - \cos \phi (\dot{y}_e + y_e)\} \cdot \bar{f}.\end{aligned}\quad (24)$$

In (24), three different values of \bar{f} can be chosen according to (11) (i.e., depending on the values of $\sqrt{\bar{a}} \theta_2 - \sin \phi (\dot{x}_e + x_e) - \cos \phi (\dot{y}_e + y_e)$ and $\cos \phi (\dot{x}_e + x_e) - \sin \phi (\dot{y}_e + y_e)$).

(i) First, assume that $\sqrt{\bar{a}} \theta_2 \neq \sin \phi (\dot{x}_e + x_e) + \cos \phi (\dot{y}_e + y_e)$. Then, (24) becomes

$$\begin{aligned}\dot{V} &\leq -\{\sin \phi (\dot{x}_e + x_e) + \cos \phi (\dot{y}_e + y_e) - \sqrt{\bar{a}} \theta_2\}^2 \\ &\quad - \{\cos \phi (\dot{x}_e + x_e) - \sin \phi (\dot{y}_e + y_e)\}^2 \\ &\leq 0.\end{aligned}\quad (25)$$

Thus, V is a Lyapunov function for the x -, y -, and θ -dynamics, and the uniform asymptotic stability of the closed-loop system is achieved. Hence, $\sin \phi (\dot{x}_e + x_e) + \cos \phi (\dot{y}_e + y_e) - \sqrt{\bar{a}} \theta_2$ and $\cos \phi (\dot{x}_e + x_e) - \sin \phi (\dot{y}_e + y_e)$ continue decreasing until they become zero (Hong, 1997).

(ii) Second, assume that $\sqrt{\bar{a}} \theta_2 = \sin \phi (\dot{x}_e + x_e) + \cos \phi (\dot{y}_e + y_e)$ and $\cos \phi (\dot{x}_e + x_e) + \sin \phi (\dot{y}_e + y_e) \neq 0$. Then, firstly (22) becomes

$$\dot{V}_2 \leq -\bar{a} \theta_2^2, \quad (26)$$

and thus, $\sqrt{\bar{a}} \theta_2$ and also $\sin \phi (\dot{x}_e + x_e) + \cos \phi (\dot{y}_e + y_e)$ become bounded. And, secondly (19) becomes

$$\begin{aligned}\dot{V}_1 &= -(\dot{e} + e)^T (\dot{e} + e) + \sqrt{\bar{a}} \theta_2 \cdot \{L \sin \theta (\dot{\phi})^2 + \sqrt{\bar{a}} \theta_2 \\ &\quad + \text{sgn}(\theta_2) \cdot |\sin \phi (2\dot{x}_e + \dot{x}_e) + \cos \phi (2\dot{y}_e + \dot{y}_e)|\}.\end{aligned}\quad (27)$$

Hence, from (26), (17) is uniformly asymptotically stable, and thus, from (27), (15) and (16) are input-to-state stable (i.e., input θ_2 and state $\dot{e} + e$). Then, the interconnected system (15) through (17) is also uniformly asymptotically stable (Khalil, 2002).

(iii) Third, the given conditions are

$$\sin \phi (\dot{x}_e + x_e) + \cos \phi (\dot{y}_e + y_e) - \sqrt{\bar{a}} \theta_2 = 0, \quad (28)$$

$$\cos \phi (\dot{x}_e + x_e) - \sin \phi (\dot{y}_e + y_e) = 0. \quad (29)$$

The time derivative of (29) becomes

$$\begin{aligned}\{-\sin \phi (\dot{x}_e + x_e) - \cos \phi (\dot{y}_e + y_e)\} \cdot \dot{\phi} \\ + \{\cos \phi (\ddot{x}_e + \dot{x}_e) - \sin \phi (\ddot{y}_e + \dot{y}_e)\} = 0.\end{aligned}\quad (30)$$

(15) and (16) yields:

$$\cos \phi (\ddot{x}_e + 2\dot{x}_e + x_e) = \sin \phi (\ddot{y}_e + 2\dot{y}_e + y_e). \quad (31)$$

Also, subtracting (29) from (31) yields:

$$\cos \phi (\ddot{x}_e + \dot{x}_e) = \sin \phi (\ddot{y}_e + \dot{y}_e). \quad (32)$$

Hence, equation (30) becomes

$$\{\sin \phi (\dot{x}_e + x_e) + \cos \phi (\dot{y}_e + y_e)\} \cdot \dot{\phi} = 0. \quad (33)$$

Thus, the following two cases can be obtained: a) $\sin \phi (\dot{x}_e + x_e) + \cos \phi (\dot{y}_e + y_e) = 0$ or b) $\dot{\phi} = 0$. In the case of a), (28) gives $\theta_2 = 0$, (29) yields $(\dot{x}_e + x_e)^2 + (\dot{y}_e + y_e)^2 = 0$, and (24) reduces to $\dot{V} \leq 0$. Also, the second equation in (20) becomes

$$\dot{\theta}_2 = -\bar{c} \sin(\theta_1), \quad (34)$$

because $-\bar{a} \theta_2 + \{\sin \phi (2\dot{x}_e + \dot{x}_e) + \cos \phi (2\dot{y}_e + \dot{y}_e)\} - \sqrt{\bar{a}} \cdot \bar{f} = 0$. Hence, $\theta_1 = 0$ follows from (34). In the case of b), (15), (16), and $\dot{\phi} = 0$ yield:

$$\begin{aligned}\sin \phi (\ddot{x}_e + 2\dot{x}_e + x_e) + \cos \phi (\ddot{y}_e + 2\dot{y}_e + y_e) \\ = \sqrt{\bar{a}} \theta_2 + \sin \phi \dot{x}_e + \cos \phi \dot{y}_e\end{aligned}\quad (35)$$

$$\sin \phi (\ddot{x}_e + \dot{x}_e + x_e) + \cos \phi (\ddot{y}_e + \dot{y}_e + y_e) = \sqrt{\bar{a}} \theta_2 \quad (36)$$

By (28) and (36), it follows that

$$\sin \phi \ddot{x}_e + \cos \phi \ddot{y}_e = 0. \quad (37)$$

Also, the time derivative of (28), (37), and $\dot{\phi} = 0$ give

$$\sin \phi \dot{x}_e + \cos \phi \dot{y}_e = d(\sqrt{\bar{a}} \theta_2) / dt. \quad (38)$$

Now, combining the time derivative of (38), (37), and $\dot{\phi} = 0$, it follows that

$$d^2(\sqrt{\bar{a}} \theta_2) / dt^2 = 0 \quad (39)$$

from which (34) can be used to have

$$\begin{aligned}d^2(\cos \theta_1 \cdot \theta_2) / dt^2 \\ = -\theta_2 (\cos \theta_1 \cdot \theta_2^2 - 3\bar{c} \sin^2 \theta_1 + \bar{c} \cos^2 \theta_1) \\ = 0.\end{aligned}\quad (40)$$

Thus, either $\theta_2 = 0$ or $\cos \theta_1 \cdot \theta_2^2 - 3\bar{c} \sin^2 \theta_1 + \bar{c} \cos^2 \theta_1 = 0$ follows. In the latter case, the quadratic formula gives $\cos \theta_1 = (-\theta_2^2 + \sqrt{\theta_2^4 + 48\bar{c}^2}) / 8\bar{c} \geq 0$, whose solution (θ_1, θ_2) should also satisfy (34) since (34) holds in the case of b) as well. However, it can be easily seen that this leads to a contradiction. Therefore, $\theta_2 = 0$ follows from (40), and thus, $\theta_1 = 0$ from (34).

In both cases a) and b), $\theta_1 = \theta_2 = 0$ are obtained, and thus, $\dot{x}_e + x_e = \dot{y}_e + y_e = 0$ from (28) and (29). Note that (24) reduces to $\dot{V} \leq 0$ in any case. \square

4. SIMULATIONS AND EXPERIMENTS

First, computer simulations of three control laws (i.e., the PD and E^2 control laws of (Fang, *et al.*, 2003), and the proposed nonlinear control law in Section 3), using equations (3)-(4), were carried out. The system parameters used in the simulations were

$$\begin{aligned}m_p = 0.73 \text{ kg}, m_t = 1.06 \text{ kg}, m_g = 3.0 \text{ kg}, \\ I = 0.005 \text{ kg m}^2, L = 0.7 \text{ m}.\end{aligned}\quad (41)$$

The x and y position errors at the target positions and the swing angle throughout traveling were compared. Even though a performance comparison with various

payload weights and initial sway angles was performed, the discussion in this paper is limited to the case of $m_p = 0.73$ kg and $\theta(0) = 0$ deg, because similar behaviors were observed in other cases. The target positions of the trolley and girder were

$$[x_d, y_d]^T = [1.0, 1.0]^T. \quad (42)$$

Also, simulations with various target positions besides (4) were pursued, but the overall trend was the same.

Fig. 2 shows the simulation results of the PD control in equation (6), where the used gains are $k_d = 102$, $k_p = 45$, and $k_E = 1$. The positioning control of the trolley and girder according to (42) is acceptable (see Fig. 2a,b), but, even though their target positions had been achieved at about 9 sec, the payload continues oscillating (see Fig. 2c). Fig. 3 depicts the simulation results of the E^2 control in (7), where the used gains are $k_d = 125.3$, $k_p = 50$, and $k_E = 0.001$. Compared with Fig. 2, the set-point regulation is almost the same, but the θ -oscillation has been much improved (see Fig. 3c). Fig. 4 shows the simulation results of the proposed control in (8)-(11). Compared with the PD and E^2 control laws, both set-point regulation and sway suppression are much superior.

The experimental results of the three control laws using a 3-D pilot crane were also compared. The 3-D crane utilized was an InTeCo 3DCrane. As shown in Fig. 1, it consists of a trolley, a girder, and a payload hanging on a pendulum-like lift-line wound

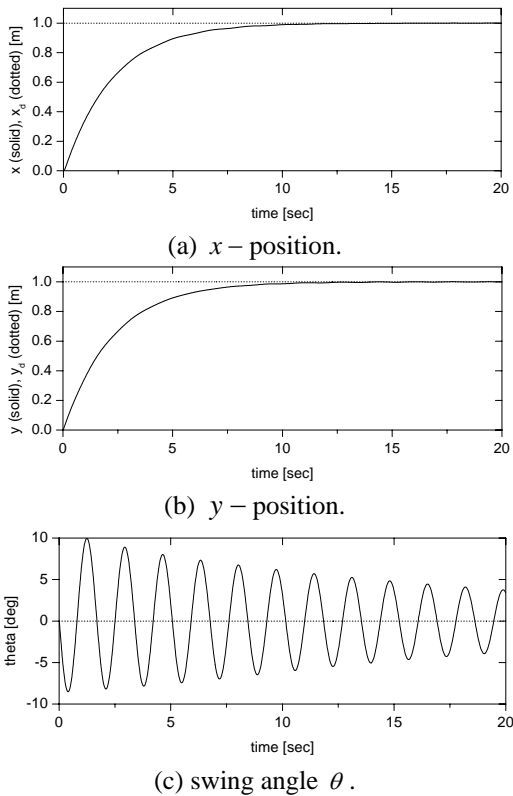


Fig. 2. Simulation result of the PD control of equation (6) with $k_d = 102$, $k_p = 45$, and $k_E = 1$ (dotted : target values, solid : simulation values).

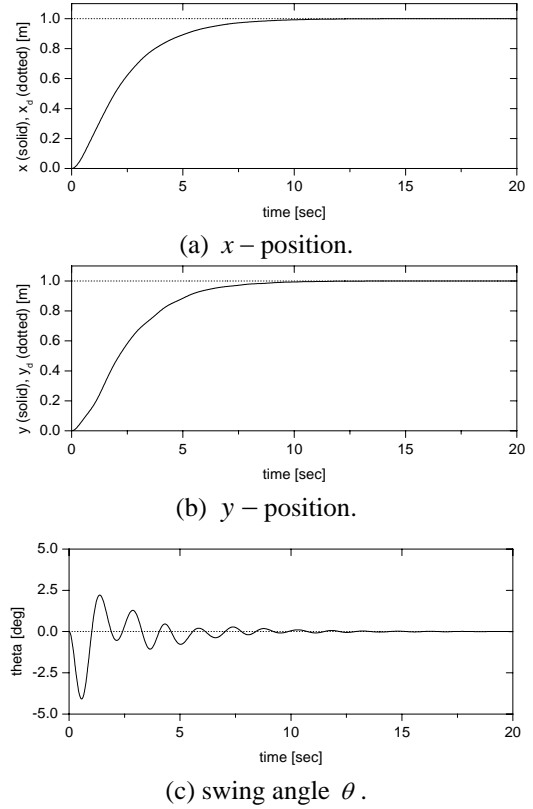


Fig. 3. Simulation result of the E^2 control of (7) with $k_d = 125.3$, $k_p = 50$, and $k_E = 0.001$ (dotted : target values, solid : simulation values).

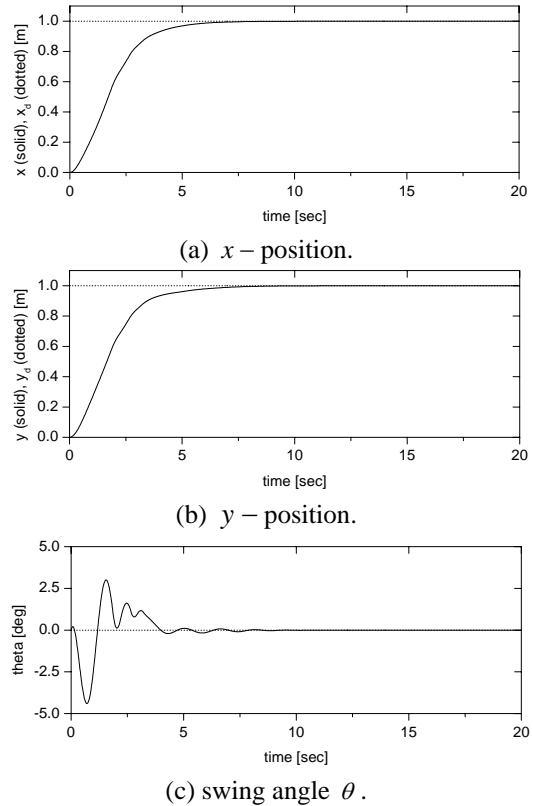


Fig. 4. Simulation result of the proposed nonlinear controller of (8)-(11) (dotted : target values, solid : simulation values).

by a motor mounted on the trolley. The girder is capable of rectilinear motion in the Y-direction, while the trolley is capable of rectilinear motion along the girder in the X-direction. The 3DCrane is driven by three DC motors. There are five encoders to measure five variables: the trolley and girder displacements, the lift-line length, and the two deviation angles of the payload (all five encoders are identical). The trolley and girder motors are driven by power interfaces, which amplify the signals from PC to DC motors and transmit the pulse signals of the encoder after converting them to 16-bit digital signals. The PC communicates with the power interface board via an internally equipped RT-DAC multipurpose digital I/O board. The physical parameters of the 3DCrane are given in (41). Actually, the 3DCrane values were used in simulations for comparison purposes. The sampling time was 0.01 sec. The desired target position was the same as (42).

Fig. 5 compares the experimental results of the three controllers (PD, E^2 , and the proposed one) using the same initial conditions. The rise time of the E^2 control and that of the proposed one are almost the same, but the better sway suppression characteristics of the proposed controller are shown.

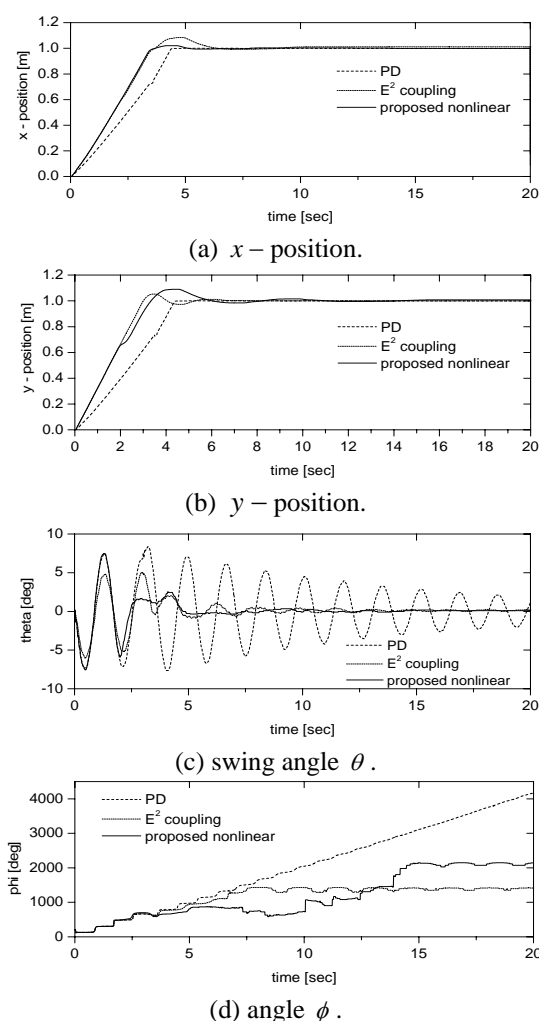


Fig. 5. Experiment results(PD, E^2 , proposed control).

5. CONCLUSIONS

In this paper, a nonlinear control law for 3-D overhead cranes using the feedback linearization technique and the decoupling strategy of θ - and ϕ -dynamics from x - and y -dynamics was investigated. The performance of the proposed controller was compared with those of the PD and E^2 control laws of (Fang, *et al.*, 2003). The stability proof in this paper is much more rigorous than those available in the literature. Because most transferences of loads in factories are performed with a fixed rope length, the applicability of the proposed controller is very high. The question of changing the rope length remains for future work.

ACKNOWLEDGMENT

This work was supported by the Ministry of Science and Technology of Korea under a program of the National Research Laboratory, grant number NRL M1-0302-00-0039-03-J00-00-023-10.

REFERENCES

- Agostini, M.J., G.G. Parker, H. Schaub, K. Groom, and R.D. Robinett III (2003). Generating swing-suppressed maneuvers for crane systems with rate saturation. *IEEE Transactions on Control Systems Technology*, **11**(4), 471-481.
- Butler, H., G. Honderd and J. Van Amerongen (1991). Model reference adaptive control of a gantry crane scale model. *IEEE Control Systems Magazine*, **11**(1), 57-62.
- Fang, Y., W.E. Dixon, D.M. Dawson and E. Zergeroglu (2003). Nonlinear coupling control laws for an underactuated overhead crane system. *IEEE/ASME Transactions on Mechatronics*, **8**(3), 418-423.
- Hong, K.S. (1997). Asymptotic behavior analysis of a coupled time-varying system: application to adaptive systems. *IEEE Transactions on Automatic Control*, **42**(12), 1693-1697.
- Hong, K.S., B.J. Park and M.H. Lee (2000). Two-stage control for container cranes. *JSME International Journal, Series C*, **43**(2), 273-282.
- Khalil, H.K. (2002). *Nonlinear systems*. 3rd edition, Prentice-Hall.
- Kiss, B., J. Levine and Ph. Mullhaupt (2000). A simple output feedback PD controller for nonlinear cranes. *Proceedings of the IEEE Conf. Decision and Control*, 5097-5101.
- Manson, G.A. (1977). *Time Optimal Control Methods Arising from the Study of Overhead Cranes*, Ph.D. thesis, University of Strathclyde, Glasgow, U.K.
- Moustafa, K.A.F. and A.M. Ebeid (1988). Nonlinear modeling and control of overhead crane load sway. *Journal of Dynamic Systems, Measurement, and Control*, **110**, 266-271.